www.ietdl.org

Published in IET Communications
Received on 6th September 2012
Revised on 12th March 2013
Accepted on 21st April 2013
doi: 10.1049/iet-com.2012.0811

ISSN 1751-8628

Low-complexity channel estimation and turbo equalisation for high frequency channels

Qiang Li[1], *Kah Chan Teh*[2], *Kwok Hung Li*[2]

[1]*National Key Laboratory of Science and Technology on Communications, University of Electronic Science and Technology of China, Chengdu 611731, People's Republic of China*
[2]*INFINITUS Infocomm Centre of Excellence, School of EEE, Nanyang Technological University, Singapore*
E-mail: ekhli@ntu.edu.sg

Abstract: A low-complexity channel estimation algorithm is proposed to improve performance of two high frequency standardised waveforms: MIL-STD-188-110B Appendix C standard and STANAG 4285. In the proposed estimation algorithm, the channel impulse response is modelled as a linear-time function within a frame and the least square criterion is adopted. With the estimated CIRs, the authors study and compare bit-error-rate (BER) performance and complexity of three turbo equalisation (TEQ) schemes, including the minimum mean-square error (MMSE), the MMSE with decision feedback equalisation (DFE) (MMSE-DFE) and the soft-feedback interference-cancellation (SFIC) turbo receivers. The authors then propose a hybrid TEQ scheme that uses the MMSE-DFE equaliser for the first iteration and the SFIC equaliser for the rest. Simulation results show that the proposed channel estimation algorithm performs well and the TEQ schemes realise a significant performance improvement as compared with a non-iterative receiver. Moreover, the proposed hybrid TEQ scheme achieves the best trade-off between BER and complexity for the MIL-STD-188-110B Appendix C standard, whereas the SFIC-TEQ scheme is optimal for the STANAG 4285 standard.

1 Introduction

For high frequency (HF) communications, the MIL-STD-188-110B Appendix C standard [1] and the STANAG 4285 norm [2] are popular HF waveforms recommended by the USA and North Atlantic Treaty Organisation, respectively. In the subsequent description, these standards are referred to as MIL-STD and STANAG for simplicity. The frequently adopted HF channel model is ITU-R F.1487 channel model. HF channels suffer from fast time variation and large delay spread, resulting in severe time-varying inter-symbol interference (ISI).

Turbo equalisation (TEQ) [3, 4] is an effective technique to mitigate ISI. Recently, TEQ has been adopted by wireless communications [5], underwater acoustic communications [6, 7], optical fibre communications [8] and cooperative communication systems [9]. Both the soft-in soft-out (SISO) equaliser and SISO decoder are required for TEQ. In practice, a linear equaliser or a decision feedback equalisation (DFE) is commonly used as the SISO equaliser, since optimal equalisers, such as maximum a posteriori probability (MAP) estimators, are too complicated to implement. Accordingly, Tuchler and Singer [4] proposed a linear minimum mean-square error (MMSE) filter with time-varying filter coefficients. In [10], the authors replaced the optimal equaliser with a soft-interference canceller. In [11], a soft-feedback interference-cancellation (SFIC)-based equaliser was proposed and its complexity depends only linearly on the channel memory length.

If the channel estimation is perfect, reduced-complexity TEQ schemes will achieve good performance. However, it is very difficult to achieve a perfect estimation for an HF channel in practice. In [12], a minimax scheme and a competitive scheme were studied, which incorporated the uncertainty in channel information to equaliser design in order to improve robustness. Although in [13], a doubly selective fast-fading channel was estimated using a fixed-lag Kalman filter, which is followed by a zero-phase low-pass filter, functioning as a smoother. However, these schemes increase again the complexity of TEQ algorithms. Adaptive algorithms, such as recursive least square (RLS) [10] and least-mean square (LMS) algorithms [14], are thus proposed to track the channel variations for each frame. Unfortunately, these algorithms do not work well under the ITU-R F.1487 HF channel conditions, mainly because of error propagation in updating the time-varying channel coefficients.

In [15], the authors proposed an least square (LS)-based method with linear interpolation to estimate the time-varying channel coefficients accurately, where the channel impulse response (CIR) of the fast fading channel is modelled as a linear function of time within a frame. An LS-based method was then proposed for time-varying channel estimation. It eliminates the need for a adaptive-tracking algorithm and the associated error floor.

In the existing HF waveform standards, separate equalisation and decoding are used at the receiver. This leads to poor bit-error-rate (BER) performance. In this

paper, we incorporate turbo receivers to improve BER performance for the conventional HF standards. However, because of the fast time variation and large delay dispersion of HF channels, optimal channel estimation methods and SISO equalisation algorithms are not feasible in practical implementation. In addition to high level modulation constellation in both HF standards, we have also investigated practical applications of some low-complexity adaptive channel estimation methods and SISO equalisers. More specifically, we first compare adaptive LMS, RLS and LS-based linear-time interpolation channel estimation algorithms. Simulation results have shown that both LMS and RLS algorithms perform poorly over HF channels. Therefore we choose the LS-based linear time interpolation channel estimation algorithm. Most importantly, no data feedback is needed for the chosen algorithm, thus the estimation algorithm is just needed to be performed once.

Furthermore, we have also studied and compared various low-complexity equalisation algorithms, such as MMSE, MMSE-DFE and SFIC algorithm. In addition, we have also analysed their computational loads. Based on this analysis, we further propose a hybrid turbo receiver to achieve the best tradeoff between computational complexity and BER performance. Numerical results show that TEQ schemes can significantly improve the BER performance as compared to that of a non-iterative receiver. Moreover, the proposed hybrid TEQ scheme achieves the best trade-off between BER and complexity for the MIL-STD standard with 8PSK, in which the complex matrix inversion operation is only required during the first iteration. On the other hand, the SFIC-TEQ scheme is the best choice for the STANAG standard with 8PSK, where only linear operations are necessary.

The rest of this paper is organised as follows. In Section 2, the two HF waveforms and their frame structures are described. In Section 3, we present the proposed LS-based linear time interpolation channel estimation algorithm and study its MSE performance. In Section 4, we study several low-complexity TEQ schemes and compare their BER performance with the proposed channel estimation method. Comparison of implementation complexity among various TEQ schemes are presented in Section 5 and a new hybrid TEQ scheme is also proposed. The conclusion is given in Section 6.

2 System description

In Fig. 1, the block diagram of a baseband HF waveform is depicted. At the transmitter, a convolutional encoder with a constraint length of seven is used to encode information bits. The encoded bits are fed into an interleaver. Specifically, it is a block interleaver for the MIL-STD standard and a convolutional interleaver for the STANAG standard. Multiple interleaving lengths have been defined in both standards. In this paper, we restrict ourselves to the case of the 'very long' interleaving length, that is, there are 72 frames for the MIL-STD standard and 10.24 s for the STANAG standard. After puncturing, the resulting code rate is 3/4 and 2/3, respectively, for the MIL-STD and STANAG standards. Coded bits are then interleaved with a scrambling sequence generated by the scrambler. The resulting sequence is mapped to an 8PSK Gray mapping constellation. The frame structures of both standards are shown in Fig. 2. For the MIL-STD standard, an initial 287-symbol preamble is followed by 72 frames of alternating data and known symbols. Each data frame contains a data block consisting of 256 data symbols, followed by a mini-probe consisting of 31 symbols of known data. All the preamble symbols, known symbols and data symbols are chosen from an 8-PSK constellation. In the STANAG standard, the symbols to be transmitted are structured in recurrent frames with a frame duration of 106.66 ms. A frame consists of 256 symbols, which can be broken down into 80 synchronisation symbols, 48 reference symbols and 128 data symbols. The 176 reference and data symbols are scrambled by a scrambling sequence with eight phase states of length 176. The synchronisation sequence uses binary PSK modulation and the modulation rate is equal to 2400 bauds. The reference and data symbols are divided into four blocks: the first three blocks consist of 32 data symbols followed by 16 reference symbols and the last block consists of 32 data symbols. All the reference symbols are represented by the symbol 0.

The modulated data sequence is passed through an ITU-R F.1487 LM channel model. This model is symbol-spaced and a delay spread of five symbol intervals (2.1 ms) is used instead of the 2.0 ms defined for the channel. The channel consists of two independent Rayleigh fading taps with a Gaussian fading spectrum affected by a 2σ Doppler spread of 1 Hz. The additive white Gaussian noise (AWGN) is also considered.

The received signal can be expressed as

$$r_n = \sum_{l=0}^{L-1} h_n(l) x_{n-l} + z_n \tag{1}$$

where L is the CIR length and z_n is zero-mean AWGN with variance σ_z^2. In addition, x_n is the transmit symbol and

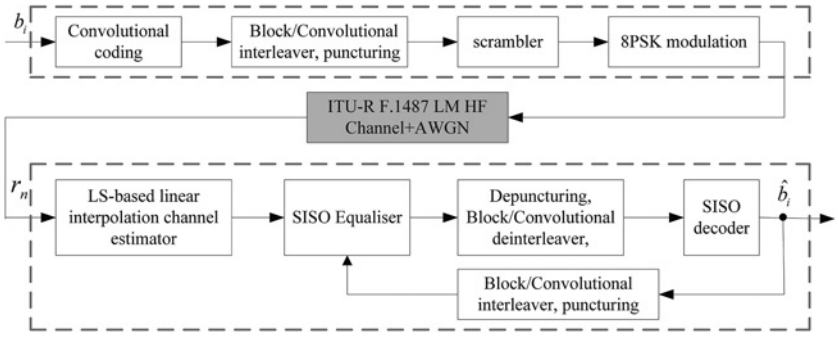

Fig. 1 *Block diagram of the baseband HF waveforms*

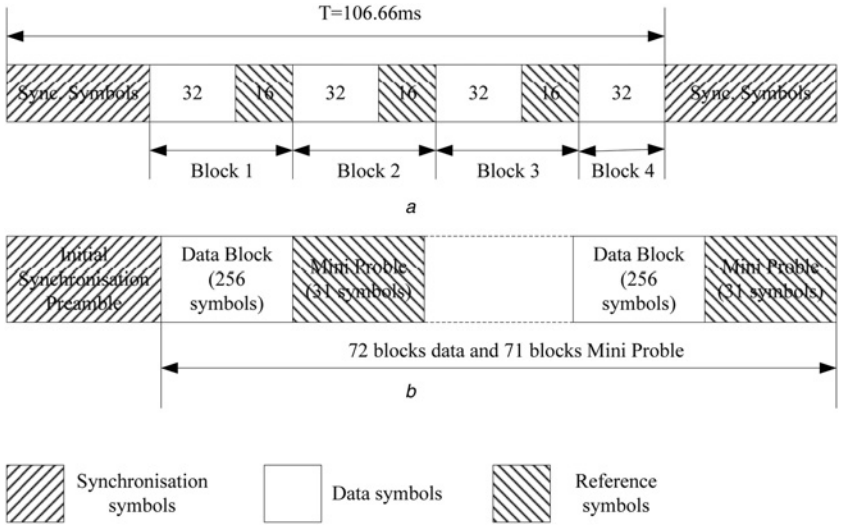

Fig. 2 *Frame structures of both HF standards*
a STANAG 4285
b MIL-STD-188-110B Appendix C

$h_n(l)$, for $l = 0, 1, \ldots, L-1$, are the zero-mean complex Gaussian time-varying CIRs.

3 LS-based linear time interpolation channel estimation

The channel estimation algorithm is similar for both standards except the frame structures are different. Therefore we just take the STANAG standard as an example to explain the algorithm.

The CIR $h_n(l)$ is expressed as a linear function of time n given by

$$h_n(l) = u_0(l) + nu_1(l) \tag{2}$$

where $u_0(l)$ and $u_1(l)$ are the $2L$ parameters to be estimated in each frame. From (1) and (2), the received signal r_n can be rewritten as

$$r_n = \boldsymbol{x}_n(\boldsymbol{u}_0 + n\,\boldsymbol{u}_1) + z_n \tag{3}$$

where $\boldsymbol{x}_n = [x_n, x_{n-1}, \ldots, x_{n-L+1}] \in C^{1\times L}$ is the transmitted vector, and $\boldsymbol{u}_j = [u_j(0), u_j(1), \ldots, u_j(L-1)] \in C^{L\times 1}$ for $j = 0,1$. With the known training symbols, the received samples contributed by the training symbols can be written into a matrix format given by

$$\boldsymbol{r} = \begin{bmatrix} \boldsymbol{A} & \boldsymbol{T}\,\boldsymbol{A} \end{bmatrix} \begin{bmatrix} \boldsymbol{u}_0 \\ \boldsymbol{u}_1 \end{bmatrix} + \boldsymbol{z} \tag{4}$$

where (see (5) and (6))

$$\boldsymbol{A} = \begin{bmatrix} x_{L-1} & x_{L-2} & \cdots & x_1 & x_0 \\ \vdots & & \vdots & & \vdots \\ x_{79} & x_{78} & \cdots & x_{79-L+2} & x_{79-L+1} \\ x_{112+L-1} & x_{112+L-2} & \cdots & x_{113} & x_{112} \\ \vdots & & \vdots & & \vdots \\ x_{127} & x_{126} & \cdots & x_{127-L+2} & x_{127-L+1} \\ x_{160+L-1} & x_{160+L-2} & \cdots & x_{161} & x_{160} \\ \vdots & & \vdots & & \vdots \\ x_{175} & x_{174} & \cdots & x_{175-L+2} & x_{175-L+1} \\ x_{208+L-1} & x_{208+L-2} & \cdots & x_{209} & x_{208} \\ \vdots & & \vdots & & \vdots \\ x_{223} & x_{222} & \cdots & x_{223-L+2} & x_{223-L+1} \\ x_{256+L-1} & x_{256+L-2} & \cdots & x_{257} & x_{256} \\ \vdots & & \vdots & & \vdots \\ x_{335} & x_{334} & \cdots & x_{335-L+2} & x_{335-L+1} \end{bmatrix} \in C^{(213-5L)\times L} \tag{7}$$

and $\boldsymbol{T}$ is a diagonal matrix defined as

$$\begin{aligned} \boldsymbol{T} = \operatorname{diag}\{&L-1, \ldots, 79, 112+L-1, \ldots, 127, \\ &160+L-1, \ldots, 175, 208+L-1, \ldots, 223, \\ &256+L-1, \ldots, 335\} \end{aligned} \tag{8}$$

$$\boldsymbol{r} = \begin{bmatrix} r_{L-1} \cdots r_{79} & r_{112+L-1} \cdots r_{127} & r_{160+L-1} \cdots r_{175} & r_{208+L-1} \cdots r_{223} & r_{256+L-1} \cdots r_{335} \end{bmatrix}^{\mathrm{T}} \in C^{(213-5L)\times 1} \tag{5}$$

$$\boldsymbol{z} = \begin{bmatrix} z_{L-1} \cdots z_{79} & z_{112+L-1} \cdots z_{127} & z_{160+L-1} \cdots z_{175} & z_{208+L-1} \cdots z_{223} & z_{256+L-1} \cdots z_{335} \end{bmatrix}^{\mathrm{T}} \in C^{(213-5L)\times 1} \tag{6}$$

doi: 10.1049/iet-com.2012.0811

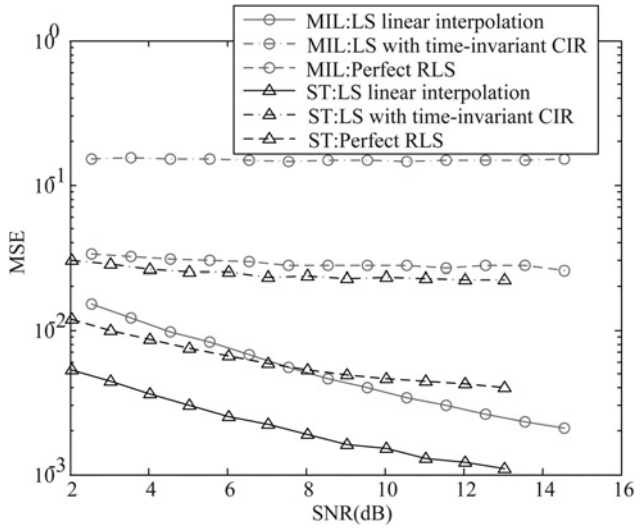

Fig. 3 *MSE of various channel estimation algorithms against SNR*

According to [15], based on the LS criterion, the estimated $\hat{\boldsymbol{u}} = \left[\hat{\boldsymbol{u}}_0^{\mathrm{T}} \hat{\boldsymbol{u}}_1^{\mathrm{T}}\right]^{\mathrm{T}}$ can be derived as

$$\hat{\boldsymbol{u}} = \begin{bmatrix} \boldsymbol{A}^H\boldsymbol{A} & \boldsymbol{A}^H\boldsymbol{T}\boldsymbol{A} \\ \boldsymbol{A}^H\boldsymbol{T}\boldsymbol{A} & \boldsymbol{A}^H\boldsymbol{T}^2\boldsymbol{A} \end{bmatrix}^{-1} \begin{bmatrix} \boldsymbol{A}^H\boldsymbol{r} \\ \boldsymbol{A}^H\boldsymbol{T}\boldsymbol{r} \end{bmatrix} \tag{9}$$

Using the matrix-inversion lemma, we compute $\hat{\boldsymbol{u}}$ recursively [15]. With the estimation of the parameters $\hat{\boldsymbol{u}}_0$ and $\hat{\boldsymbol{u}}_1$, the CIRs of the entire frame can be obtained from (2).

Fig. 3 depicts the time-average MSE versus signal-to-noise ratio (SNR) computed by various channel estimation algorithms under the ITU-R F.1487 LM channel profile. The channel fading is assumed to be independent from block to block. As the HF channels suffer from fast time variation and large delay dispersion instead of block fading, it is very complex to use the optimal channel estimation algorithm to evaluate and track HF channel coefficients. Thus, in this paper, we consider several low-complexity channel estimation algorithms. To highlight the advantage of the LS-based linear time interpolation algorithm for HF channels, we use the term 'perfect RLS' as a reference. In the perfect RLS algorithm, it is assumed that the data symbols are known. Actually, when the number of pilots is large enough, the RLS algorithm performs close to 'perfect RLS'. It can be seen that for both standards, the LS-based linear-time interpolation algorithm has the smallest average MSE as compared with that of the other two algorithms. We observe that as the SNR increases, the average MSE of the proposed algorithm decreases faster than that of the LS algorithm without the channel tracking and the perfect RLS algorithm.

Table 1 Number of required operations per pilot and data symbols using varying channel-estimation algorithms, where L Is the CIR length

	LS	RLS	Proposed method
pilot symbol	$6L^2+3L/5L^2$	$6L^2+3L/5L^2$	$4(6L^2+3L)-6L/4(5L^2)$
data symbol	0/0	$6L^2+3L/5L^2$	L/L

On the other hand, we can see that the average MSE of each algorithm for the standardization agreement (STANAG) waveform is smaller than that of the corresponding one for the MIL-STD waveform. This is because there are more pilot symbols embedded in the STANAG waveform.

An important aspect of the channel-estimation algorithms is their computational complexity. In the following, we consider the LS algorithm (without channel tracking), the proposed LS-based linear-time interpolated method, and the adaptive RLS algorithm for comparison as all of the algorithms employ the LS estimator.

Table 1 shows the required number of real multiplications and additions per pilot, and data symbols to estimate the CIR. In this table, X in X/Y denotes the required number of real multiplications, whereas Y denotes the required number of real additions. The LS and RLS require $6L^2+3L$ real multiplications and $5L^2$ real additions per pilot symbol, and the proposed method requires about four times as much as that of the LS algorithm. To track the time-varying channel using the data symbols, the LS method has no extra operations, since the CIR is assumed constant for the entire burst. The RLS algorithm requires the same number of computation operations as for the pilot symbols. However, the proposed method requires only L real multiplications and L real additions in updating the CIR for the data symbols. We need to highlight that the proposed algorithm only needs to perform once while the RLS algorithm needs to perform one time during each iteration.

It is shown that the the proposed method can effectively combat the Doppler frequency up to 300 Hz. Since the maximum Doppler frequency in both standards is less than 10 Hz, we do not present the corresponding simulation results in this paper.

Since the LS-based linear-time interpolation channel estimation algorithm gives better performance for the two HF waveform standards, we will adopt it in the TEQ receivers.

4 Low-complexity TEQ schemes and their performance

Both the SISO equaliser and the SISO decoder are important components for TEQ receivers. Since a log-MAP algorithm is normally used to decode data, in this section, we explore several low-complexity SISO equalisation algorithms. In the following descriptions for equalisation algorithms, the estimated CIRs instead of perfect CIRs are used.

4.1 Linear SISO MMSE equaliser

The linear MMSE equaliser processes a length-N window of observations $\boldsymbol{r}_n = \left(r_{n-N_2} r_{n-N_2+1} \cdots r_{n+N_1}\right)^{\mathrm{T}}$, $N = N_1 + N_2 + 1$, to compute the estimated symbol $\hat{x}_n$. We assume that the transmitted symbols x_n are circularly symmetric, thus we can omit the pseudovariance. Following that, the estimates $\hat{x}_n$ can be computed as

$$\begin{aligned} \hat{x}_n &= \frac{\boldsymbol{f}_n^H\left(\boldsymbol{r}_n - \boldsymbol{H}_n\bar{\boldsymbol{x}}_n\right) + \bar{x}_n s_n}{1 + \left(1 - v_n\right)s_n} \\ \boldsymbol{f}_n &= \left(\sigma^2\boldsymbol{I}_N + \boldsymbol{H}_n\boldsymbol{V}_n\boldsymbol{H}_n^H\right)^{-1}\tilde{\boldsymbol{h}}_n \\ s_n &= \boldsymbol{f}_n^H\tilde{\boldsymbol{h}}_n \end{aligned} \tag{10}$$

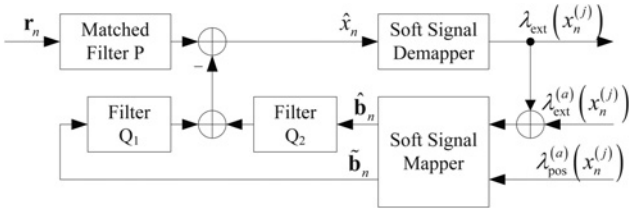

Fig. 4 *Principle block diagram of the SFIC-based equaliser*

where $\boldsymbol{V}_n = \text{diag}\left[v_{n-L-N_2+1} v_{n-L-N_2+2} \cdots v_{n+N_1}\right]$, in which v_n is the variance of the feedback symbol at the previous iteration, $\bar{\boldsymbol{x}}_n = \left(\bar{x}_{n-N_2-L+1} \bar{x}_{n-N_2-L+2} \cdots \bar{x}_{n+N_1}\right)^{\text{T}}$, in which $\bar{x}_n$ is the mean of each feedback symbol, and

$$\boldsymbol{H}_n = \begin{bmatrix} \boldsymbol{h}_n & 0 & \cdots & 0 \\ 0 & \boldsymbol{h}_n & \cdots & 0 \\ & & \ddots & \\ 0 & \cdots & 0 & \boldsymbol{h}_n \end{bmatrix} \tag{11}$$

$$\boldsymbol{h}_n = \left[h_n(L-1) \cdots h_n(0)\right] \tag{12}$$

$$\tilde{\boldsymbol{h}}_n = \boldsymbol{H}_n \left[\mathbf{0}_{1\times(N_2+L-1)} \quad 1 \quad \mathbf{0}_{1\times N_1}\right]^{\text{T}} \tag{13}$$

Assuming that the filtered signal is Gaussian distributed, we calculate the extrinsic log-likelihood ratio (LLR), $\lambda_{\text{ext}}(x_n^{(j)})$, of the jth bit in $\hat{x}_n$ as [4] (see (14))
where $\lambda_{\text{ext}}^{(a)}(x_n^{(k)})$ is the a-prior LLR of $x_n^{(j)}$ fed back from the decoder during the previous iteration.

4.2 SISO MMSE-DFE equalisation

An MMSE-DFE equaliser consists of a length-N feedforward filter with $N = N_1 + N_2 + 1$, and a length-N_b feedback filter. To effectively remove the ISI, we choose $N_2 = 0$, $N_b = L - 1$ and $N_1 = N - 1$. Assuming that the DFE is error free and by using the MMSE criterion, we can obtain the optimal filter of the SISO MMSE-DFE equaliser which has the same form as (10) with $\boldsymbol{V}_n = \text{diag}\left[v_{n-L+1}^d \cdots v_{n-1}^d \quad v_n \quad v_{n+1} \quad \cdots v_{n+N-1}\right]$ and $\bar{\boldsymbol{x}}_n = \left(x_{n-L+1}^d \cdots x_{n-1}^d \quad x_n \cdots x_{n+N-1}\right)^{\text{T}}$. Here, x_n^d and v_n^d are the mean and variance of the past estimated symbol for the current iteration, respectively. The calculation of the soft output information for the MMSE-DFE equaliser is also identical to that of the MMSE equaliser.

4.3 SFIC equalisation

The SFIC equaliser consists of three linear filters as shown in Fig. 4. In Fig. 4, $\lambda_{\text{pos}}^{(a)}(x_n^{(j)})$ represents the decoded posterior LLR of the jth bit of x_n during the previous iteration, $\hat{\boldsymbol{b}}_n$ and $\tilde{\boldsymbol{b}}_n$ are the estimated feedback vectors. Note that filter P is a matched filter with filter coefficients $\boldsymbol{p} = \boldsymbol{h}^*$, filter Q_1 is strictly anti-causal and filter Q_2 is strictly causal. We denote their tap coefficients by $\boldsymbol{q}_1 = [q_{-L+1}, \ldots, q_{-1}]^{\text{T}}$ and $\boldsymbol{q}_2 = [q_1, \ldots, q_{L-1}]^{\text{T}}$, respectively. Note that $q_l = \sum_{i=0}^{L-1} h_n^*(i-l)\, h_n(i)$, $l \in [-L+1, \ldots, -1, 1, \ldots, L-1]$. According to [11], the equalised symbol can be expressed as

$$\hat{x}_n = \sum_{i=0}^{L-1} |h_n(i)|^2 x_n + \boldsymbol{q}_1^H(\tilde{\boldsymbol{x}}_n - \tilde{\boldsymbol{b}}_n) - \boldsymbol{q}_2^H(\hat{\boldsymbol{x}}_n - \hat{\boldsymbol{b}}_n) + \tilde{z}_n \tag{15}$$

with

$$\tilde{\boldsymbol{x}}_n = \left[x_{n+L-1}, \ \ldots, \ x_{n+1}\right]^{\text{T}} \tag{16}$$

$$\hat{\boldsymbol{x}}_n = \left[x_{n-1}, \ \ldots, \ x_{n-L+1}\right]^{\text{T}} \tag{17}$$

and

$$\tilde{\boldsymbol{b}}_n = \left[\bar{x}_{n+L-1}, \ \ldots, \ \bar{x}_{n+1}\right]^{\text{T}} \tag{18}$$

$$\hat{\boldsymbol{b}}_n = \left[\bar{x}_{n-1}, \ \ldots, \ \bar{x}_{n-L+1}\right]^{\text{T}} \tag{19}$$

where $\bar{x}_n$ denotes the mean value of the feedback symbol. It is worth noting that $\bar{x}_n$ in (18) is estimated according to $\lambda_{\text{pos}}^{(a)}(x_n^j)$, whereas $\bar{x}_n$ in (19) is predicted using this present channel information $\lambda_{\text{ext}}(x_n^{(j)})$ plus the soft output channel decoder's extrinsic information $\lambda_{\text{ext}}^{(a)}(x_n^{(j)})$. In addition, the equivalent noise term is

$$\tilde{z}_n = \sum_{i=0}^{L-1} h_n(i)^* z_{n+i} \tag{20}$$

We can compute the mean and variance of $\hat{x}_n$ as $\hat{\mu}_n(x_n) = \sum_{i=0}^{L-1} |h_n(i)|^2 x_n$ and $\hat{v}_n = \boldsymbol{q}_1^H \text{diag}\{1 - \tilde{\boldsymbol{b}}_n\}\boldsymbol{q}_1 + \boldsymbol{q}_2^H \text{diag}\{1 - \hat{\boldsymbol{b}}_n\}\boldsymbol{q}_2$, respectively. Assuming $\hat{x}_n$ is a Gaussian distributed variable, we can calculate its output LLR as (see (21))
Using these SISO equalisation algorithms, we carry out simulations to evaluate the BER performance of TEQ schemes for both HF waveforms over ITU-R F.1487 LM channels. The channel fading is assumed to be independent from block to block. From the simulations, we observe that the TEQ receiver with the RLS channel estimation algorithm does not converge for a few frames because of a significant estimation error. Therefore we do not present the

$$\lambda_{\text{ext}}(x_n^{(j)}) = \ln \frac{\sum_{x_n : x_n^{(j)}=0} \exp\left(-\left(\left(|\hat{x}_n - x_n|^2\right)/\left(1 - s_n/\left(1 + (1 - v_n)s_n\right)\right)\right)\right) \prod_{k \neq j} \exp\left(-x_n^{(k)} \lambda_{\text{ext}}^{(a)}(x_n^{(k)})\right)}{\sum_{x_n : x_n^{(j)}=1} \exp\left(-\left(\left(|\hat{x}_n - x_n|^2\right)/\left(1 - s_n/\left(1 + (1 - v_n)s_n\right)\right)\right)\right) \prod_{k \neq j} \exp\left(-x_n^{(k)} \lambda_{\text{ext}}^{(a)}(x_n^{(k)})\right)} \tag{14}$$

$$\lambda_{\text{ext}}(x_n^{(j)}) = \ln \frac{\sum_{x_n : x_n^{(j)}=0} \exp\left(-\left(\left(|\hat{x}_n - \hat{\mu}_n(x_n)|^2\right)/(\hat{v}_n)\right)\right) \prod_{k \neq j} \exp\left(-x_n^{(k)} \lambda_{\text{ext}}^{(a)}(x_n^{(k)})\right)}{\sum_{x_n : x_n^{(j)}=1} \exp\left(-\left(\left(|\hat{x}_n - \hat{\mu}_n(x_n)|^2\right)/(\hat{v}_n)\right)\right) \prod_{k \neq j} \exp\left(-x_n^{(k)} \lambda_{\text{ext}}^{(a)}(x_n^{(k)})\right)} \tag{21}$$

doi: 10.1049/iet-com.2012.0811

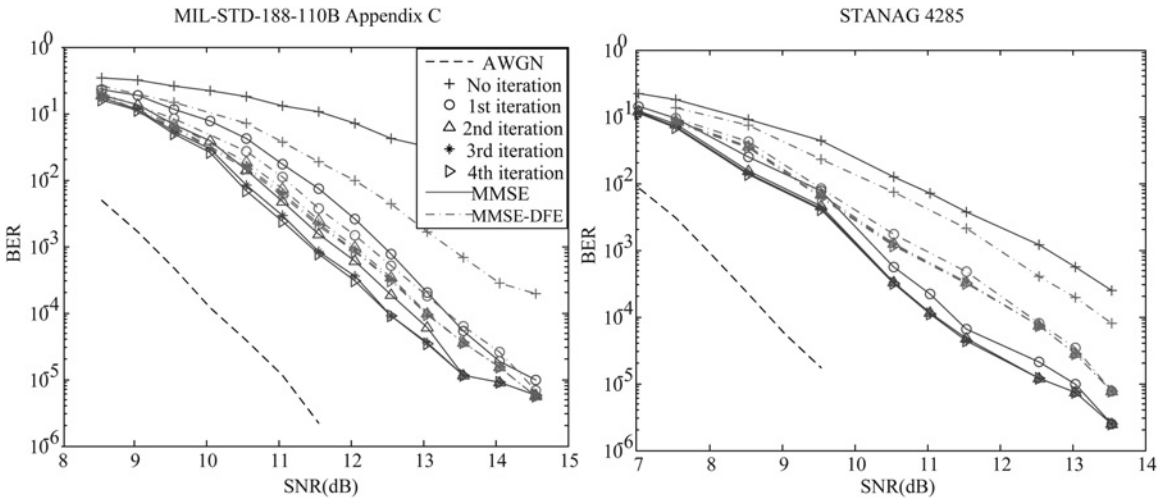

Fig. 5 *Performance comparison between the MMSE and the MMSE-DFE-TEQ schemes over ITU-R F.1487 LM channels*

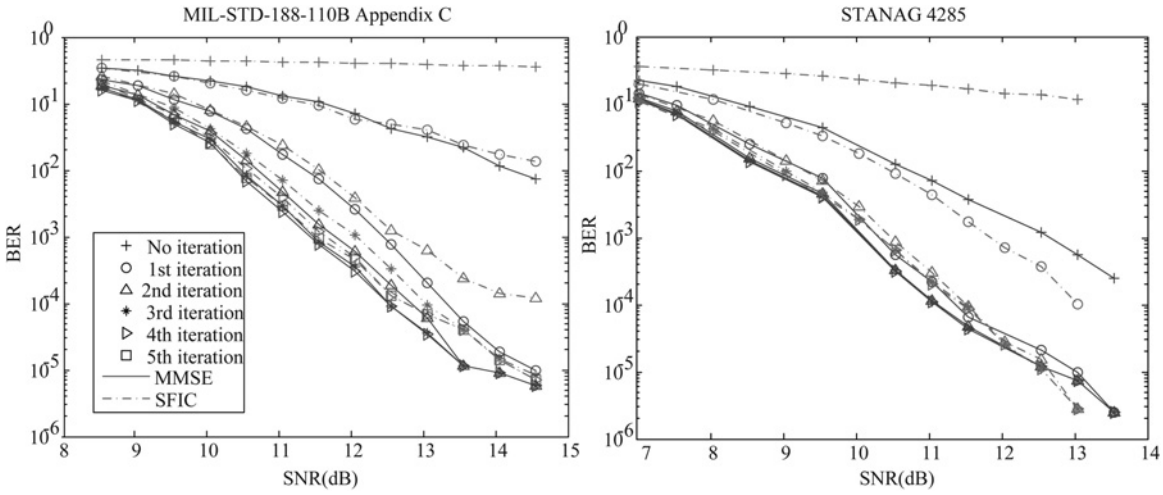

Fig. 6 *Performance comparison between the MMSE and the SFIC-TEQ schemes over ITU-R F.1487 LM channels*

BER performance of TEQ receivers with a RLS channel estimator here. Instead, the LS-based linear time interpolation channel estimation algorithm is adopted for all simulations. Fig. 5 shows the BER performance comparisons between the MMSE-TEQ and MMSE-DFE-TEQ schemes. The filter length is set to $N = 20$ for both receivers, and 15 precursor and 5 postcursor taps are employed for the SISO equaliser. The interleaving length is 72 frames for the MIL-STD standard and 10.24 s for the STANAG standard, respectively. From Fig. 5, we can conclude: (i) for the STANAG standard, the required SNR to achieve a certain BER over an ITU-R F.1487 LM channel is lower by more than 1 dB for the MMSE-DFE TEQ as compared to the DFE-based receiver, whereas the iterative gain is at least 2 dB for the MMSE equalisation algorithm. Moreover, we observe that the SNR gains after iterations are more significant for the MIL-STD standard; (ii) the MMSE-TEQ scheme outperforms the MMSE-DFE-TEQ scheme after convergence, whereas it is the opposite for the case without iterations; (iii) there is a 2–3 dB performance loss for these TEQ schemes with respect to the case of no ISI; and (iv) for an ITU-R F.1487 LM channel, 1 iteration (i.e. two times equalisation and decoding) is enough for the STANAG waveform, whereas the other waveform requires 1 iteration and 2 iterations for the MMSE-DFE-TEQ scheme and the MMSE-TEQ scheme, respectively.

In Fig. 6, we present the simulation results using the SFIC-TEQ scheme over ITU-R F.1487 LM channels. It shows that the SFIC-TEQ scheme has comparable BER performance as the MMSE-TEQ scheme after convergence. However, the BER performance is very poor at the initial stage because of severe ISI resulting from a matching filter without any a priori information. In addition, the required number of iterations is 2 for the STANAG waveform, while it is 3 for the other one.

5 Complexity analysis and the proposed hybrid-TEQ scheme

The turbo receiver consists of two components, namely, the equaliser and the decoder. For different schemes, only the equaliser is different, whereas the log-MAP algorithm is used in the decoder for all the schemes. For an 8-PSK constellation and an ITU-R F.1487 LM channel, it has the

Table 2 Operations in units of equivalent additions required per received symbol per iteration using various SISO equalisation algorithms

Algorithm	MMSE/MMSE-DFE	SFIC
operation	$24N^2 + 6L^2 - 14N + 12L$	$8L^2 + 26L - 24$

Table 3 Operations in units of equivalent additions required by various TEQ schemes for the STANAG 4285

Algorithm	MMSE	MMSE-DFE	SFIC	Hybrid
number of iterations	1	1	2	1
operations	16 994	16 994	11 709	12 400

Table 4 Operations in units of equivalent additions required by various TEQ schemes for the MIL-STD-188-110B Appendix C

Algorithm	MMSE	MMSE-DFE	SFIC	Hybrid
number of iterations	2	1	3	1
operations	23 890	15 926	15 612	11 866

parameter values of $q = 8$, $L = 6$ and $N = 20$, where q, L and N denote the alphabet size of the constellation, CIR length and the number of filter taps, respectively. We assume that the statistics $\bar{x}_n$ and v_n of x_n are available for all n and we do not consider the computation of $\lambda_{\text{ext}}(x_n^{(j)})$. Any overhead due to initialisation (one-time operations for all iterations) is neglected. Moreover, in this analysis, we do not include memory read/write and the number of memory required, because the memory management is very dependent on the programming and implementation method. The number of required real-valued operations (multiplications or additions) per received symbol per iteration of the several algorithms mentioned above are shown in Table 2. Note that the matrix inversion operations in the MMSE and the MMSE-DFE equalisers are implemented through a fast time-recursive update algorithm introduced in [16]. In addition, we assume that the transmitted symbols x_n are circularly symmetric, so that the pseudovariances can be discarded. With the given code rate and the modulation level, the equivalent complexity per information bit per iteration is 1/2 and 4/9 times of that per symbol per iteration for the STANAG and MIL-STD waveforms, respectively. On the other hand, the complexity of the log-MAP decoder is $(4p + 50) \times 2^M - 19$ per bit per iteration, where the encoder memory length is $M = 6$, and the code rate is $1/p = 1/2$. Evidently, the number of iterations has significant influence on the total computational load. Tables 3 and 4 show the total operations per bit for both standards.

To achieve better trade-off between complexity and BER performance, we propose a new hybrid TEQ (hybrid-TEQ) scheme. In this scheme, the MMSE-DFE equalisation is adopted for the first iteration, and the SFIC algorithm is used for the subsequent iterations. This is because the MMSE-DFE scheme produces better performance without a priori information.

Fig. 7 shows the BER performance of the proposed hybrid-TEQ scheme. It is observed that this scheme can converge after 1 iteration. Accordingly, it has comparable performance with the MMSE-TEQ after convergence. At BER = 10^{-4}, the SNR improvement exceeds 2 dB. The required number of operations for the TEQ algorithm are shown in Tables 3 and 4.

It can be observed that the SFIC-TEQ scheme has the least computational load for the STANAG waveform; however, the hybrid-TEQ scheme is the simplest for the MIL-STD waveform. In general, these low-complexity TEQ schemes still perform well.

Note that for MMSE and MMSE-DFE algorithms, since the channel is time variant, we update the coefficient vector and compute the estimates $\hat{x}_n$ for each n. We can further simplify their complexity by assuming that the coefficient vector is approximately time invariant during a short period of time at the cost of some performance loss.

In summary, we first estimate CIRs using the LS-based linear-time interpolation algorithm, which is just needed to be performed once before performing the TEQ algorithms. With the estimated CIRs, we carry out the SFIC-TEQ algorithm for the STANAG standard, and perform the proposed hybrid-TEQ algorithm for the MIL-STD waveform iteratively until a predefined maximum number of iterations.

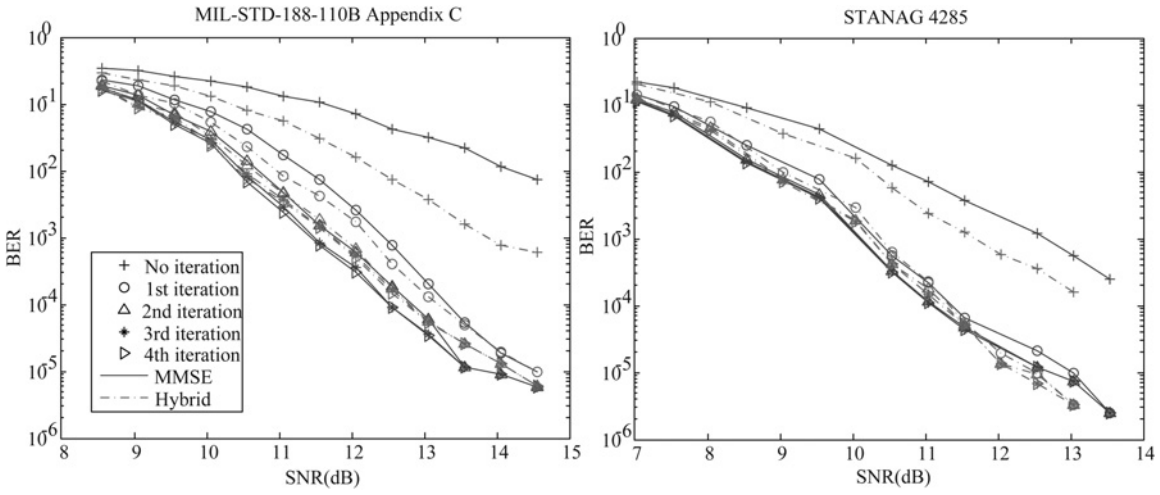

Fig. 7 *Performance comparison between the MMSE and the hybrid schemes over ITU-R F.1487 LM channels*

doi: 10.1049/iet-com.2012.0811

6 Conclusion

In this paper, we have investigated practical applications of several low-complexity channel estimation algorithms and TEQ schemes for both HF waveform standards. We have also proposed a new hybrid-TEQ scheme. It has been shown that conventional LMS and RLS channel estimation algorithms perform poorly over ITU-R F.1487 LM channel models. However, the LS-based linear-time interpolation estimation algorithm is a suitable choice for these models. Moreover, this estimation algorithm is only executed once. As expected, TEQ schemes can significantly improve the BER performance of a non-iterative receiver. In terms of the tradeoff between the BER performance and the achievable complexity, the proposed hybrid-TEQ scheme is a good candidate scheme for the MIL-STD-188-110B Appendix C waveform, whereas the SFIC-TEQ is suitable for the STANAG 4285 waveform.

7 References

1 Department of defense interface standard: 'Interoperarability and performance standards for data modem', April 2000
2 North Atlantic Treaty Organization: 'Characteristics of 1200/2400/3600 bits per second single tone modulators/demodulators for HF radio links', Feburary 1989
3 Yang, P., Ge, J.H.: 'Combination of turbo equalization and turbo trellis coded modulation with low complexity', *IET Commun.*, 2007, **1**, (4), pp. 772–775
4 Tuchler, M., Singer, A.C.: 'Turbo equalization: an overview', *IEEE Trans. Inf. Theory*, 2011, **57**, (2), pp. 920–952
5 Qin, Z., Teh, K.C.: 'Reduced-complexity turbo equalization for coded intersymbol interference channels based on local search algorithms', *IEEE Trans. Veh. Technol.*, 2008, **57**, (1), pp. 630–634
6 Walree, P.V., Leus, G.: 'Robust underwater telemetry with adaptive turbo multiband equalization', *IEEE J. Ocean. Eng.*, 2009, **34**, (4), pp. 645–655
7 Wan, H., Chen, R.R., Choi, J.W., Singer, A., Preisig, J., Farhang, B.B.: 'Markov chain Monte Carlo detection for underwater acoustic channels'. Proc. Inf. Theory Applications Workshop, January 2010, pp. 1–5
8 Xu, F., Khalighi, M.A., Bourennane, S.: 'Coded PPM and multipulse PPM and iterative detection for free-space optical links', *IEEE J. Opt. Commun. Netw.*, 2009, **1**, (5), pp. 404–415
9 Gong, Y., Ding, Z., Ratnarajah, T., Cowan, C.F.N.: 'Turbo channel estimation and equalization for a superposition-based cooperative system', *IET Commun.*, 2009, **3**, (11), pp. 1790–1799
10 Lopes, R., Barry, J.: 'The soft-feedback equalizer for turbo equalization of highly dispersive channels', *IEEE Trans. Commun.*, 2006, **54**, (5), pp. 783–788
11 Vogelbruch, F., Haar, S.: 'Low complexity turbo equalization based on soft feedback interference cancelation', *IEEE Commun. Lett.*, 2005, **9**, (7), pp. 586–588
12 Nargiz, K., Suleyman, K., Alper, T.E.: 'Robust turbo equalization under channel uncertainties', *IEEE Trans. Signal Process.*, 2012, **60**, (1), pp. 261–273
13 Alireza, M., Michael, M.G.: 'Estimation of fast-fading channels for turbo receiver with high-order modulation', *IEEE Trans. Veh. Technol.*, 2013, **62**, (2), pp. 667–678
14 Chen, J., Wang, Y.: 'Adaptive MLSE equalizers with parametric tracking for multipath fast fading channels', *IEEE Trans. Commun.*, 2001, **49**, (4), pp. 655–663
15 Leong, S.Y., Wu, J.X., Xiao, C.S., Olivier, J.C.: 'Fast time-varying dispersive channel estimation and equalization for an 8-PSK cellular system', *IEEE Trans. Veh. Technol.*, 2006, **55**, (5), pp. 1493–1502
16 Tuchler, M., Singer, A., Koetter, R.: 'Minimum mean squared error equalization using priors', *IEEE Trans. Signal Process.*, 2002, **50**, (3), pp. 673–683